

Scientific Computing

Spread of infectious disease

MAXIMILIAN HECKER

Date of publication: 08.08.2023

Contents

1	Introduction	2
2	Theory	2
3	Methodology	3
4	Implementation	3
4.1	Grid-parsing	3
4.2	Random numbers	4
4.3	Code functionality	4
5	Results and Discussion	5
5.1	Goodness of randomly generated numbers	5
5.2	Average infection rates	5
5.2.1	Infection rate depending on probability of infection	6
5.2.2	Infection rate depending on probability of vaccination	8
6	Suitability of the algorithm	9
7	Appendix	10
7.1	Hotspot-spreading	10
8	References	11
9	Attachments	12
9.1	Statistical fluctuations in small grids	12
9.2	Visual spread propagations	12

1 Introduction

In order to counteract the spread of infectious diseases among a society, it is pivotal to understand the spread dynamics accurately. Therefore it is of interest finding certain models that can handle the dynamics properly. Unlike many other physical models, the spread of infectious diseases cannot be considered a deterministic development. Instead, it follows a stochastic propagation. When one contagious person is exposed to a group of susceptible persons, the transmission of the virus or bacterium follows probabilistic rules. It depends on the infection probability which itself determines the so-called *basis reproduction number* R_0 of an epidemic. This factor represents the infections caused by one contagious case in an non-immune population and is a crucial number to quantify the rapidity of the spread, and consequently its aggressiveness in real-world scenarios [3]. Based on the infection probability and further likelihoods for recovery and regaining susceptibility after an infection, a probabilistic model can be devised describing the development realistically.

A convenient indicator for the severity of a disease-spread is the time-average of the infection rate, meaning the average percentage of a society being contagious. Ultimately, this factor is influenced by various dynamic changes of the epidemic and can represent the behaviour elaborately. The simulation will primarily focus on analysing dynamic changes resulting from both probabilistic and general system variations. In the following, the average infection rates over time as functions of specific probabilities are examined and conclusions regarding the system's dynamics as well as the model suitability will be drawn.

2 Theory

The spread of an infectious disease - being a stochastic process - is modelled using transfer-probabilities. Depending on the current health-state, a person is likely to change its status with a certain probability. These probabilities are formulated in the following model-rules. The spread dynamics are influenced by

- The probability of infection if exposed to a contagious neighbour, p_1 .
- The probability of recovery after having sustained an infection, p_2 .
- The probability of becoming susceptible when fully recovered, p_3 .
- The probability of being vaccinated and therefore immune, p_4 .

It is crucial to notice here that the probability of infection does not remain exactly p_1 if more than one neighbour is contagious. In fact, the infections are independent events which makes it more likely receiving the disease if more neighbours are infected. Since the probabilities are independent and the order of events is not regarded, the probability is formulated by the binomial distribution.[5] The likelihood of an successful infection is given by

$$p(\text{'Infected'}) = \sum_{k=1}^n \binom{n}{k} \cdot p_1^k (1-p_1)^{n-k} = 1 - (1-p_1)^n \quad (1)$$

where n denotes the number of infected neighbours. In words: the risk is the counter-probability of n infection-failures.

The dynamic of the spread is quantified and assessed using the average infection rate over time. It is determined by first calculating the infection rate (2) for each time point t . The infection rate represents the current number of infected cells out of all cells. Eventually, the time-averaged mean (3) is calculated. Mathematically:

$$\langle I \rangle_t = \frac{1}{L^2} \sum_{n=0}^{L^2} I_n \quad \overline{\langle I \rangle} = \frac{1}{\Delta t} \sum_{t=0}^{T_{\max}} \langle I \rangle_t \quad (2, 3)$$

The average infection rate is a measure of the contamination of a society across a time-span Δt . This metric will be front and center when discussing the spread dynamics and is the core of the examination.

3 Methodology

Since the development of an infectious disease is not a deterministic process, it cannot reasonably be described using differential equations and physical laws. Instead it is necessary to implement an algorithm which statistically represents the dynamics. A convenient method is the utilization of an *cellular automaton*.

A cellular automaton is a multidimensional grid of cells (here it will be two-dimensional). Each of these cells can assume one of multiple states (also referred to as status) upon which they are classified. These can be either numerical or categorial.[8]. The time dynamics are computed by updating the grid for every time step dt according to certain rules (see 2) which are explicitly predefined and oftentimes static throughout the process. However, this depends on the specific context. Potentially, a vaccination could be engineered at a later timestamp in the simulation and affect the infection dynamics in delay.

Generally, the grid can be updated either in sequential order iterating over the cells in loops, or by randomly passing through the grid updating the cells with a statistical frequency. Both approaches are feasible, though the statistical approach will prove to be more eligible within the experimental setup (see implementation 4). After a cell has been randomly selected, the algorithm takes the neighbourhood into account. Based on the states of the neighbours and on the probabilistic rules, it updates the status of the cell accordingly. The neighbourhood can be designed versatilely. The most common neighbourhoods are the *Moore* neighbourhood which encompasses all directly adjacent cells as well as the diagonally adjacent neighbours, and the *Von-Neumann* neighbourhood which only regards the directly adjacent cells in the cardinal directions[2] (see figure 1).

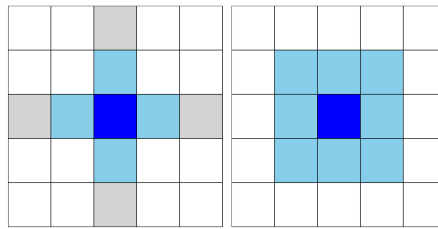


Figure 1: (left) Depiction of Von-Neumann neighbourhood considering the cardinal directions. The gray cells can potentially be considered. (right) Moore neighbourhood considering all directly and indirectly adjacent cells

4 Implementation

4.1 Grid-parsing

The two main approaches to update the grid are

- Sequentially iterating through the grid updating the cells in order
- Randomly passing through the grid updating the cells with statistical frequency

With respect to the experiment setup, which involves a dynamic (probabilistic) spread of a disease, the statistical realization is the appropriate approach. This is attributed to the decentralized and random fashion behaviour of the disease transmission. If the grid was updated in sequential order, the propagation must be assumed to suffer from severe spatial bias. Since cells updated earlier can spread the disease to their neighbours before those neighbours are updated themselves, the sequential parsing would lead to highly unrealistic outcomes and disturb the spread pattern significantly. Intuitively, the spread can be expected to have an intrinsic tendency evolving towards the direction in which the grid is sequentially renewed.

These artifacts can be spared using the statistical approach. The algorithm selects and updates cells randomly and therefore does not suffer from bias. It accurately adheres to the random nature of the spread.

4.2 Random numbers

In order to update the grid randomly and address the random nature of the process, random grid indices must be drawn. Therefore random numbers are generated using the *GSL*-library which provides various mathematical algorithms [4]. For the purpose of the simulation, the MERSENNE TWISTER MT19937 algorithm [7] is applied which will prove worthwhile with respect to a high level of randomness and sufficiently low bias (see section 5.1).

The generator is initialized by allocating the MT19937 algorithm and setting a specific seed, enabling traceability of computations. Typically, the seed corresponds to the current machine-time for simplicity. However, it can be manually set to a consciously chosen value for active replicability. Subsequently, the generator is passed to the functions where random numbers are used. When the `main` returns ultimately, the allocated random generator is freed.

4.3 Code functionality

Initially, a two-dimensional grid of size $L \times L$ is allocated and initialized using the `void initialize` method. Every cell of the grid is assigned to a health status, namely SUSCEPTIBLE, INFECTED, RECOVERED and VACCINATED. This is realized by an *enum*¹ containing all health states. Each grid-cell is a *Structure* (named `status`) which can include one element of the *enum*. The health states are randomly allocated with equal probabilities when initializing the grid in the first place. The calculation of the time development is facilitated by a `while`-loop running from $t = 0$ to $t = T_{\max}$. The loop iteratively calls an grid-update stepper (`void grid_step`) renewing the states of the cells for every time-step. The stepper is constructed as follows:

Since the grid is randomly parsed, a sufficient update density must be granted. If too many cells are spared at every function call, the dynamic would be profoundly disturbed and not simulated accurately. Hence, the number of cell-updates must be statistically even over the grid area. It is advantageous to update L^2 cells per time-step.

Following, a random number between 0 and $L^2 - 1$ is drawn, representing an random index in a flattened grid of length L^2 . The corresponding row and column index of the two-dimensional grid is calculated utilizing the grid's symmetry. Subsequently, the cell is updated according to the model-rules. If the cell is susceptible, a function named `count_infected_neighbours` analyses the *Von-Neumann* neighbourhood of the identified cell. It examines how many neighbours are contagious and can therefore spread the disease, and eventually returns the number. Conditional on the number of infected neighbours, the probability of infection p is then determined according to (1) in the `calc_probability` function. The considered cell becomes contagious if a randomly drawn number q between 0 and 1 fulfills $q \leq p_1$. To respect the edges of the grid and not run into an issue when checking for a non-existing neighbour, an additional zero-padding of width one is appended to the grid, broadening the dimension to $(L + 2) \times (L + 2)$. In every loop iteration the infection rate (2) is calculated. When T_{\max} is reached, the average infection rate over time (3) is determined. These computations are conducted for varying probabilities and grid sizes, and ultimately printed to a file. The respective parameters (probabilities, grid-sizes etc.) are stated in the `main` of the code for best possible clarity.

The computational cost arises from generating random numbers and examining the neighbourhood. Both the generation and the examination of the neighbourhood requires $O(1)$. Since the `grid_step` function is called L^2 times, the computational cost adds up to $O(L^2)$. Thus, the statistical approach scales quadratically with the grid size L .

The computation time typically does not exceed a few seconds for every simulation (for one grid size L). However, since the dependencies for a variation of probabilities and grid sizes are examined, the entire code takes approximately 3 minutes to finish.

¹An enum (short for enumerated type) contains a finite number of named variables. They act as identifiers and are therefore constants within the code[1].

5 Results and Discussion

5.1 Goodness of randomly generated numbers

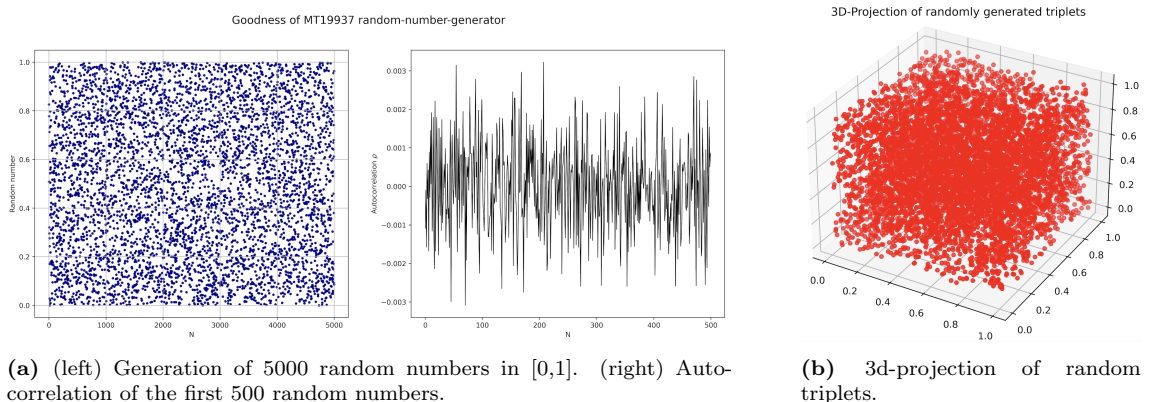
A precise simulation and realistic results can only be obtained, if the probabilistic calculations are based upon a genuinely random generation of numbers. Therefore the goodness of the randomness must be evaluated before the simulation can be considered convincing. Two possible methods are

- Auto-correlating an array of randomly generated numbers
- Plotting triplets of random numbers in a 3D-plot and identifying potential hyper-planes

The auto-correlation is the correlation of a signal with itself at a previous index. Conventionally, it refers to a signal at a prior point in time. If the signal underlies a specific generative bias, meaning that the generation follows a mathematical function and therefore shows a periodic pattern, then the auto-correlation would ideally reveal the concealed pattern [6]. The more arbitrary the auto-correlation, the better the generated numbers.

The second method is tightly related to the auto-correlation and yields a better visualisation for the goodness. Triplets of random numbers are drawn respectively and plotted in a 3d-projection. It is related to the auto-correlation insofar as a pattern in the generative model will result in recognizable hyper-planes in the 3D-Plot.

For the evaluation of the goodness, an array of 5000 numbers is created using the MT19937 algorithm and passed to the `auto_correlation` method in the code. Moreover, a triplet-function is called passing 60000 random numbers in triplets. The results can be seen in figure 2a and 2b. Not only does the auto-correlation exhibit arbitrary fluctuations² and thereby indicate a high level of randomness, but equally does the 3d-projection not show any hyper-planes when rotating. These observations suggest a satisfactory level of randomness.



5.2 Average infection rates

The behaviour of the simulated system can be examined by a variation of its parameters. In the present case, it is reasonable varying the probabilities upon which the cell states are determined, and the grid-size L.

It can be assumed that all people have already been in contact with each other before "entering" the grid. Consequently, the states SUSCEPTIBLE, INFECTED, RECOVERED and VACCINATED are allocated equally likely within the grid. Though, vaccination is not considered yet. The cells are declared static, meaning that people can not move within the grid. Furthermore, the lobes of the grid are isolating boundaries. A person at the edge of the grid faces a wall and cannot infect a neighbour in that direction. A circular boundary connecting the contrary side of the grid is not suitable for a planar model.

²The auto-correlation is limited to the first 500 correlations for visual clarity.

5.2.1 Infection rate depending on probability of infection

In the following the spread of the disease will be simulated for four different grid sizes:

$$L = 16, 32, 64, 150 \quad (4)$$

The last grid-size is consciously chosen to be significantly larger to evoke possible scaling effects. It can be anticipated that smaller grids suffer from more statistical noise, since sporadic deviations from the expected dynamics disproportionately carry more weight. With a sufficiently large grid, the high number of spread occurrences would effectively average out the deviations of individual random events, reducing their impact. According to the law of large numbers statistical fluctuations decrease gradually as the scale is enlarged.

For every grid the average infection rate over a time of 300 time units is calculated depending on the probability of infection p_1 which will be incremented in steps of $\Delta p_1 = 0.02$ from 0 to 1. The other probabilities are chosen as follows

Probability	Value
Infection p_1	p
Recovered p_2	0.03
Susceptible p_3	0.03
Vaccinated p_4	0.00

Table 1: Applied model probabilities

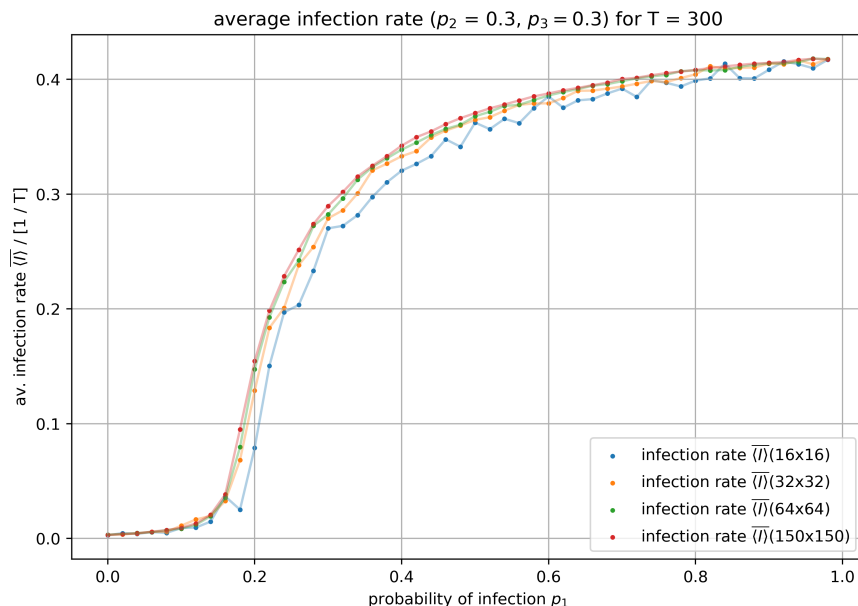


Figure 3: Average infection rate over a time of 300 time units as a function of the probability of infection p_1 . The average infection rate has been calculated for four grid-dimensions.

Evidently, more people are infected if the probability of infection is higher. With increasing probability of infection, the average infection rate over time grows exponentially at first and eventually converges towards a limit (approximately 0.42). Initially, around 33% of the people are set being contagious since the states were allocated with equal likelihood. When the probability of infection is low, the people cannot spread their disease before recovering and consequently the disease dies out quickly. The infection rate over time is then close to zero. A probability of $p_1 \approx 0.4$ indicates a equilibrium in the spread dynamics. Starting with approximately 30% infectious cells after the

initialization, the rate remains at a value 0.3 averaged over time. If p_1 exceeds this threshold, the contamination broadens and the average infection rate climbs. It is apparent that there is no critical value for p_1 where the average infection rate becomes zero. However, it is very close to zero when the probability of infection is below 0.1. Mathematically, it is impossible for the infection rate to become zero since the initialization yields a finite number of contagious people already. In order to achieve an effective extinction of the disease, counter-measures such as vaccination or social isolation, or factors like increased lethality must be considered to break the dynamics.

The figure exhibits the independence of the spread from the grid size $L \times L$ on principle. Even though the grid sizes cover a broad range, the curves are well aligned and converge towards a common limit. However, minor deviations occur: the smaller the grid, the slightly less the average infection rate. The curves seemingly approximate a well-defined "true" function with increasing grid size. Simultaneously, the statistical noise diminishes with greater L - as anticipated previously. Once passing 32x32 and proceeding, the dependency, and consequently the spread dynamic becomes more stable and robust.

To analyse the dynamics further, the probability of being recovered is adjusted to $p_2 = 0.6$. Hence, incidents in which cells recover before they can infect other cells, will emerge more frequently and the infection rate can be expected to be generally lower for the same p_1 than before. The spread might be damped. The calculations are conducted analogously for $L = [16, 32, 64, 150]$.

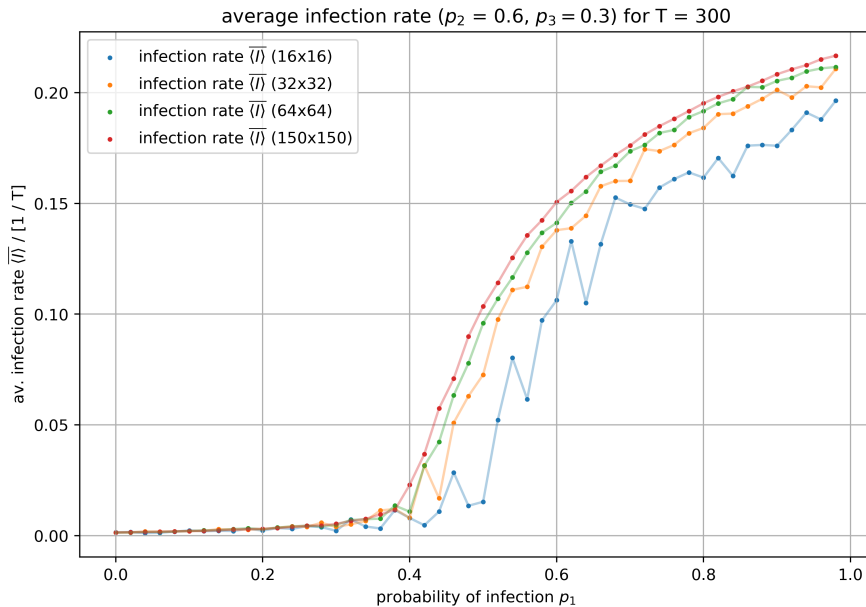


Figure 4: Average infection rate over a time of 300 time units as a function of the probability of infection p_1 . The average infection rate has been calculated for four grid-dimensions.

As estimated, the average infection rate tends to be lower for the same p_1 and the curve development delayed. The broadening of the disease is considerably obstructed by a multitude of cells recovering quickly. Consequently, the average infection rate over time consistently remains below the initial 33% infected cells following the grid's initialization. Unlike the previous scenario, the spread is mitigated for all values of p_1 . Even with an infection probability of 1, meaning a highly certain transmission of the disease, the average number of contagious cells diminishes within the grid and stabilizes at approximately 22%. This observation is visualised in figure 8. For $p_1 \leq 0.4$ the average infection rate approximates zero and the disease goes extinct. Recovery bears more on the dynamics than infections.

Consistent with the first results, the dependency becomes more defined and stable as the grid size increases. Deviations in the average infection rates can be identified even more distinctly. As

evident in the figure, the statistical fluctuations are more profound than previously. Particularly the curve for the smallest grid suffers from intense noise. This as well as the deviations in the curve trend can be attributed to the following reason:

Since the probability of recovery with $p_2 = 0.6$ is higher than before, the spread becomes more unpredictable. The interaction and transition between the infected and recovered state occurs more frequently amplifying the effects of randomness and favouring fluctuations. Moreover, a higher recovery probability implies shorter duration of infectiousness leading to more rapid changes. Greater dynamics in a shorter time frame contribute to more fluctuations. Additionally, smaller grids are more prone to noise, since outliers in the dynamic carry more weight amid a few instances. To eliminate the possibility of fluctuations arising from coding or model errors, the statistical distribution of the scattering can be examined. Each calculation of the average infection rate $\langle \bar{I} \rangle$ can be repeated multiple times, and eventually the mean and standard deviation determined. An corresponding analysis (see figure 7) reveals indeed even scattering among multiple iterations since the mean curve is sharply defined. Hence, the scattering has been averaged out implying even deviations around the mean.

5.2.2 Infection rate depending on probability of vaccination

In the following, the model is augmented by taking additional vaccination into account. If a cell is vaccinated, it is immune for the entire process of the simulation. The vaccination equally underlies a probabilistic assumption. A person is vaccinated with a certain probability p_4 which can vary from 0 to 1. Vaccinated persons are rendered immune to both receiving and transmitting the disease.

Applying this modification, a considerable change in the spread dynamics can be anticipated. Once the probability of vaccination surpasses a critical value, the disease should become extinct. This can be intuitively understood as infected people being surrounded by a critical number of vaccinated people, effectively "absorbing" the infection. Therefore the persons recover and cannot distribute their disease. When the probability of vaccination heads towards 1 in a limit case, nobody can receive the virus and the average infection rate is zero. For p_4 approaching zero, the infection rate is expected to be at its maximum for the given system settings. Thus, a monotonous decline can be anticipated.

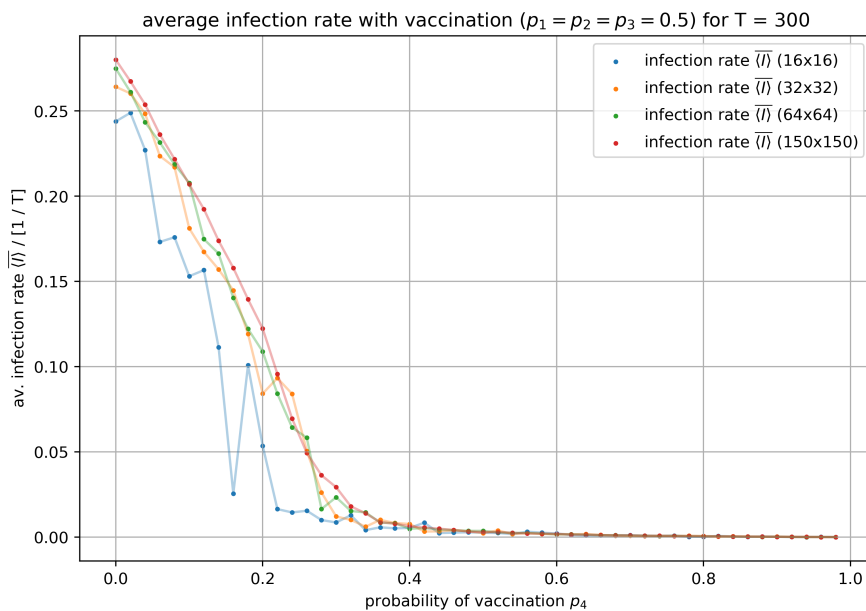


Figure 5: Average infection rate over a time of 300 time units as a function of the probability of vaccination p_4 . The average infection rate has been calculated for four grid-dimensions.

As estimated, the curve drops monotonously for soaring probability of vaccination. All curves sustain an equal trend. Similar to previous findings, the smaller grids suffer from significant stochastic noise. The figure indicates that for $p_4 = 0$ (no vaccination) the average infection rate takes a value of $\langle \bar{I} \rangle \approx 0.3$ aligning with the initial infection rate of around 33% at the time of the grid's initialization. Thus, a system building on $p_1 = p_2 = p_3 = 0.5$ yields an constant equilibrium over time. The infections remain nearly constant and the spreading stagnates. As vaccination is considered for $p_4 \geq 0$ the infection rate drops exponentially and the dynamics are mitigated. Contagious people do not encounter a sufficiently high number of susceptible neighbours to convey their disease. For $p_1 \geq 0.4$ the average infection rate approximates zero and the disease can be considered extinct. In this case, the society has surpassed a vaccination level which is considered as herd immunity. A visualisation of how the herd immunity effectively mitigates the spread is shown in figure 9. Given the aggressiveness of a disease (i.e. all the probabilities representing the disease), the necessary rate of vaccination that is critical for the herd immunity can be determined. This emphasises the importance of appropriate simulations amid real-world epidemics. It can help assessing the situation, deploying effective precautions and forecasting the dynamic.

6 Suitability of the algorithm

The algorithm as well as the conceptual assumptions underlie simplified models and therefore do not represent the spread of a contagious disease perfectly accurate. Nevertheless, the employed algorithm succeeds in modelling the random and probabilistic nature of epidemic dynamics.

One simplification lies in the assumption that the cells do not move within a time interval. For instance, the given grid could be modelling a stadium full of people at a concert, including contagious cases. In this case the dynamic of the disease would be highly affected by the dynamic of the moving people. Though, the impact of this effect strongly depends on the incubation time of the disease which corresponds to the infection probability. The higher the probability of infection, the less relevant the intern movement becomes.

Moreover, the applied algorithm assumes a *Von-Neumann* neighbourhood. Hence, only the direct neighbours in the cardinal directions are regarded as potentially contagious. More accurately, the *Moore* neighbourhood considers the diagonal neighbours as well. Though, both models are simplified models which reduce computational cost and code complexity. A precise model would encompass a broad range of neighbours since infections can be transferred omitting nearer neighbours in-between. Additionally, the probability of infection would decrease as distance does.

$$p_{i,j} = p(d_{i,j}) \quad d_{i,j}: \text{Distance between cell i and j} \quad (5)$$

Mathematically, this behaviour can be modelled using a bivariate Gaussian distribution which takes the distances of the central cell to a neighbour as the argument.

$$p_{i|j} = p_0 \cdot \exp(-d_{i,j}^2/2\sigma^2) \quad (6)$$

If the distance to another cell converges to zero, the likelihood of infection equals p_0 . With increasing distance, the probability decreases as a function of the standard deviation σ .

Furthermore, various external factors influence the process which are not directly quantifiable and therefore left out in the model. Exemplary, in a realistic scenario the susceptibility of an infection significantly depends on the strength of the individual immune system, the age of the person, possible pre-existing conditions etc. This can further lead to unexpected deaths, an extended recovery time or an decreased acceptance towards a vaccination. Though, the model is based on a homogeneous crowd of people, each being equally acceptable to any of the existing health states. Even factors unrelated to the individual do have bearings on the dynamics in a real-world scenario. Aerosol density, humidity, temperature etc. are noteworthy influences on the spread of the disease[9].

All these considerations can be generally respected when assuming the probabilities as not constant, augmenting the models complexity and thereby accuracy. One reasonable approach is to ascribe a normally distributed behaviour to the system's probabilities.

$$p \sim \mathcal{N}(p | p_0, \sigma) \quad (7)$$

All probabilities are centered around the mean μ which represents the current probability of the simplified model. The scattering is mathematically equivalent to external factors influencing the dynamic of the contamination. The higher the standard deviation σ the more perturbations are implemented in the model. This makes it more robust and realistic.

7 Appendix

7.1 Hotspot-spreading

The conducted simulation was based on a evenly distributed initialization with

$$P(\text{SUSCEPTIBLE}) = P(\text{INFECTED}) = P(\text{RECOVERED})$$

Though, in real-life epidemic proceedings, a spread is oftentimes initiated by certain hotspots, i.e. a small collective of contagious persons. This will make the dynamic more unpredictable and simultaneously creates a visually more intriguing dynamic. One implementation of hotspots is to first choose a discrete number of initially infected persons N . In the following, N random integer numbers between 0 and $L^2 - 1$ are drawn and the corresponding grid coordinates determined (similar to the grid-update stepper). Thereby, the N hotspots are positioned randomly among the grid and statistically maintain a relatively high distance to one another. The initialization is facilitated by the `initialize_hotspots` function. Following, the spread will start dynamically. The below figures present different states in time for a hotspot-spreading. The hotspots expand quickly infecting susceptible cells in every direction. The figures clearly show the stochastic behaviour of the spread dynamics encouraging the general suitability of the algorithm. Furthermore, it is evident that the propagation does not suffer from spatial bias. The probabilities are $p_1 = 0.8$, $p_2 = 0.3$, $p_3 = 0.3$, $p_4 = 0.2$.

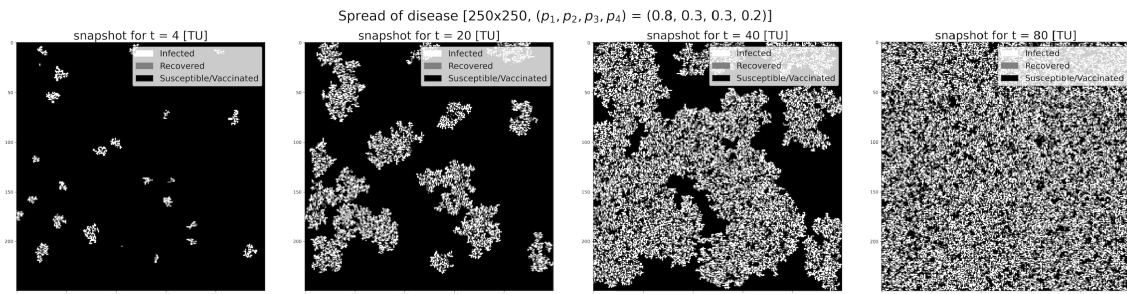


Figure 6: The image sequence depicts the time propagation of an epidemic with discrete hotspot-events. The snapshots represent the timestamps $t = [10, 20, 40, 80]$ time units

The above exhibits impressively the power of *Cellular Automata* simulating stochastic real-world developments. The grids can be dynamically adjusted to fit the spatial conditions. Borders or obstacles of any kind can be inserted, the edges can act as reflective or circular boundaries etc. Numerous possible modifications can therefore yield realistic simulations of real-world dynamics, and consequently help foreseeing future impacts.

8 References

- [1] David Bolton. What is an enum in programming languages?, thoughtco, 2023. Last accessed August 2023.
- [2] Debasis Das. A survey on cellular automata and its applications. *Communications in Computer and Information Science*, pages 97–111, 2011.
- [3] Leslie TF Yang Y Jacobsen KH Delamater PL, Street EJ. Complexity of the basic reproduction number (r_0). *Emerging Infectious Diseases*, 25:1–4, 2019.
- [4] M. Galassi et al. *GNU Scientific Library Reference Manual*, chapter ISBN 0954612078. GNU Scientif library, 3 edition, March 2016.
- [5] David Morin. *Probability: For the Enthusiastic Beginner*, chapter S.193-196, <https://scholar.harvard.edu/files/david-morin/files/chap4p.pdf>. Harvard Scholar, Boston, 1 edition, March 2016.
- [6] Mohamed N. Nounou and Bhavik R. Bakshi. Chapter 5 - multiscale methods for denoising and compression. In Beata Walczak, editor, *Wavelets in Chemistry*, volume 22 of *Data Handling in Science and Technology*, pages 119–150. Elsevier, 2000.
- [7] Ying Tan. Chapter 10 - gpu-based random number generators. In Ying Tan, editor, *Gpu-Based Parallel Implementation of Swarm Intelligence Algorithms*, pages 147–165. Morgan Kaufmann, 2016.
- [8] Eric W. Weissstein. Cellular automaton, from mathworls - a wolfram web resource, 2016. Last accessed August 2023.
- [9] World Health Organization (WHO). Communicable disease control in emergencies: a field manual, 2005. Last accessed August 2023.

9 Attachments

9.1 Statistical fluctuations in small grids

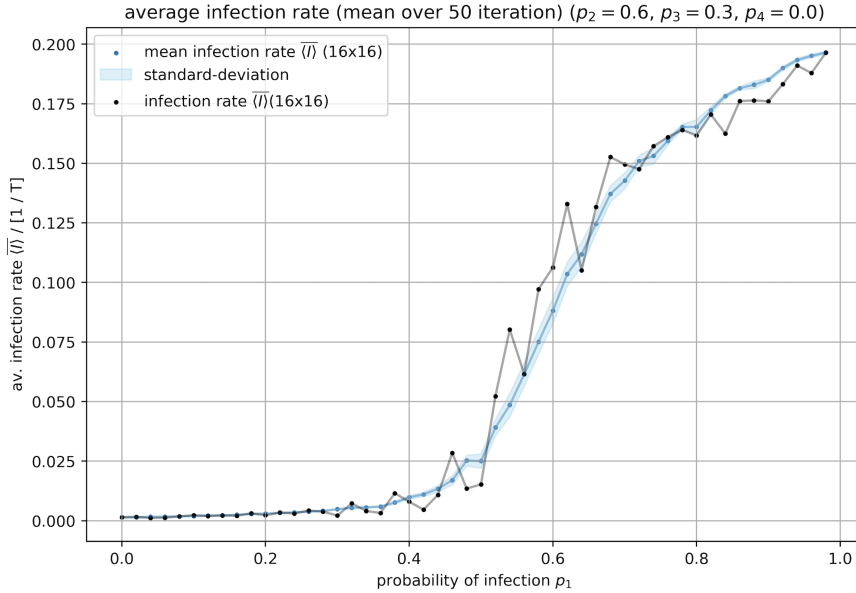


Figure 7: The figure shows the average infection rate as a function of the probability of infection p_1 for $L = 16$. The statistical fluctuations are depicted in black and the mean of 50 iterations in blue. The light-blue coating represents the standard deviation of the scattering. The mean yields a well defined curve which implies statistically even scattering around the mean.

9.2 Visual spread propagations

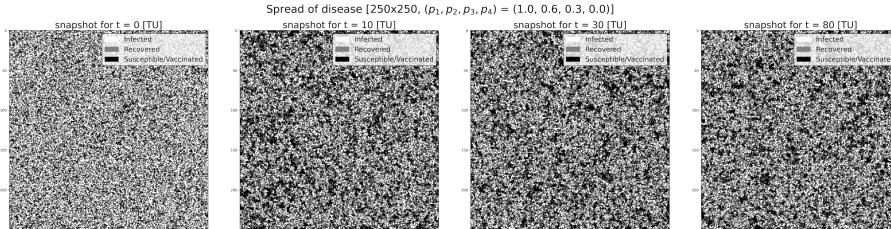


Figure 8: Spread propagation across time. The figure shows the the dynamic for $t = [0, 10, 30, 80]$ time units. The probabilities are $(p_1 = 1, p_2 = 0.6, p_3 = 0.3, p_4 = 0.0)$. Evidently, the dynamic is slightly mitigated over time.

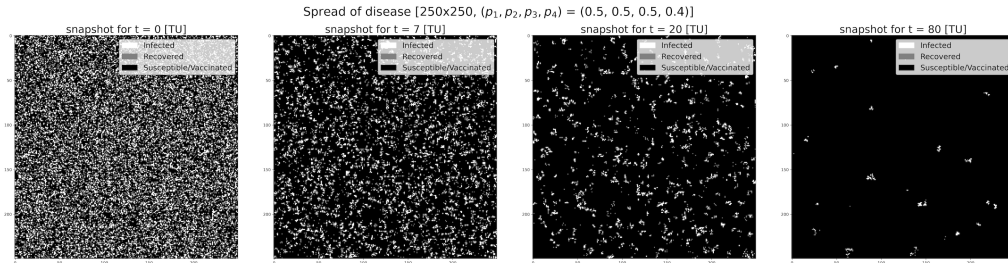


Figure 9: Spread propagation across time with vaccination included. The figure shows the dynamic for $t = [0, 7, 20, 80]$ time units. The probabilities are $(p_1 = 0.5, p_2 = 0.5, p_3 = 0.5, p_4 = 0.4)$. The average infection rate diminishes throughout time.